This paper appeared in Proceedings of the SPIE Conference on Algorithms for SAR Imagery IX, vol. 4727, Orlando, FL, April 2002.

Formation of HRR Profiles by Non-Quadratic Optimization for Improved Feature Extraction

Müjdat Çetin[a], William C. Karl[b], and David A. Castañon[b]

[a]Laboratory for Information and Decision Systems, Massachusetts Institute of Technology, 77 Massachusetts Ave., Cambridge, MA 02139, USA

[b]Multi-Dimensional Signal Processing Laboratory, Boston University, 8 Saint Mary's St., Boston, MA 02215, USA

ABSTRACT

We propose a new method for superresolution, feature-enhanced reconstruction of high range-resolution (HRR) radar profiles. We pose the problem of the formation of the HRR profiles from phase history data as an optimization problem. Resolution and feature enhancements are achieved by imposing non-quadratic regularizing constraints on the solution of the optimization problem. We present experimental results on synthetic and measured data, and compare the proposed method to currently available techniques. This analysis shows the ability of the proposed method to preserve high-resolution features such as the locations and amplitudes of the dominant scatterers in the HRR profile. This suggests that the technique may potentially help improve the performance of HRR target recognition systems.

Keywords: High range-resolution radar, feature extraction, signal reconstruction, non-quadratic optimization, superresolution.

1. INTRODUCTION

There has recently been considerable interest in using high range-resolution (HRR) radar for automatic target recognition (ATR).[1–6] The success of ATR depends on the resolution and accuracy of the target range features in the HRR profiles. Conventionally, HRR profiles are formed from the phase history data through a Fourier transform-based operation, which has a resolution limited by the radar bandwidth. Recently, high-resolution techniques have been proposed and successfully used for forming HRR profiles, and for extracting range features.[5–10]

We propose a different perspective for achieving superresolution HRR profile formation and feature extraction. We formulate the problem in a variational framework, where we minimize a regularized objective function for finding an estimate of the range profile. The key is to use appropriate non-quadratic regularizing functionals, such as ℓ_p-norms. This leads to a sparsity constraint on the reconstructed profile, and helps preserve the dominant target scatterers, while suppressing noise and clutter.

For the solution of the optimization problem posed in our framework, we use a computationally efficient Quasi-Newton scheme. We demonstrate the effectiveness of the proposed approach using examples from the University Research Initiative Synthetic Dataset (URISD),[11] and from the Moving and Stationary Target Acquisition and Recognition (MSTAR) public target data set.[12] We compare our technique to a number of methods proposed for HRR profile formation and feature extraction. The results of this study demonstrate the superresolution and accurate feature extraction capabilities of the proposed method. The approach may be of benefit for feature-based and template-based HRR ATR systems.

Further author information: (Send correspondence to M.Ç.)
M.Ç.: E-mail: mcetin@mit.edu
W.C.K.: E-mail: wckarl@bu.edu
D.A.C.: E-mail: dac@bu.edu

2. PRELIMINARIES

2.1. Context and Scope of Our Work

Conventional moving target indication (MTI) radars aim to detect, locate and track moving targets. The primary goal of HRR radars is to provide more detailed information about the observed object in order to achieve target recognition as well, while still using short dwell times. An HRR radar uses high-bandwidth pulses so that it achieves a sufficiently high resolution to profile a target. The information contained in the profile is the magnitude of the radar scattering as a function of range, along the line of sight of the radar.

There has recently been much interest in using HRR profiles for recognition of moving targets, and both template-based,[2–4] and feature-based[1] approaches to the problem have been proposed. In order for such recognition systems to be successful, the HRR profiles need to exhibit the characteristic features of the targets. Our work addresses the problem of forming HRR profiles from the observed phase history data such that important target range features are preserved, and can accurately be extracted from the HRR profile. An HRR system needs to deal with a variety of other issues prior to the target range feature extraction step, such as clutter suppression, Doppler frequency estimation, and target phase history estimation.[8] These important tasks are beyond the scope of this paper, and we concentrate on HRR profile formation and range feature extraction.

2.2. Motivation for Superresolution Processing

The primary difficulty associated with the HRR sensor for ATR is that the HRR signatures exhibit a high degree of variability. Yet, characteristic, robust features are required for successful recognition. In Ref. 1 locations and amplitudes of the dominant peaks in the HRR profile have been proposed as such features. Superresolution processing techniques for HRR profiles can help in the accurate extraction of such features, and there has been some recent work in this direction. In particular, in Refs. 7–10, a relaxation-based algorithm has been used for superresolution target feature extraction, whereas in Refs. 5, 6, the synthetic aperture radar (SAR) imaging technique of Ref. 13 has been used for forming HRR profiles. Furthermore, the study in Refs. 5, 6 has also demonstrated that superresolution techniques can improve HRR ATR performance. With these motivations, we propose a non-quadratic regularization-based superresolution signal reconstruction technique for the formation of HRR profiles.

3. SUPERRESOLUTION RECONSTRUCTION OF HRR PROFILES BY NON-QUADRATIC OPTIMIZATION

3.1. Overview

The problem we address is the inverse problem of obtaining a complex HRR profile from the received, pre-processed HRR phase history signal. To this end, let $\mathbf{x}$ be the sampled HRR profile, and $\mathbf{y}$ be the noisy sampled phase history data. Then, we have the following observation model:

$$\mathbf{y} = \mathbf{F}\mathbf{x} + \mathbf{w} \tag{1}$$

where $\mathbf{w}$ is measurement noise, and $\mathbf{F}$ is a high-resolution to low-resolution Fourier transform operator. This definition of $\mathbf{F}$ reflects the belief that the underlying object (hence its profile) possesses high-frequency features that are not captured by the resolution supported by the data. The conventional way to reconstruct the HRR profile is through an inverse Fourier transform, which, in this framework can be represented by $\hat{\mathbf{x}}_{\mathrm{CONV}} = \mathbf{F}^H\mathbf{y}$, with appropriate normalization. In contrast, we formulate the HRR profile reconstruction problem as the following optimization problem:

$$\hat{\mathbf{x}} = \arg\min_{\mathbf{x}} J_0(\mathbf{x}) \tag{2}$$

where we choose $J_0(\mathbf{x})$ to be an objective function of the following form:

$$J_0(\mathbf{x}) = \|\mathbf{y} - \mathbf{F}\mathbf{x}\|_2^2 + \lambda\|\mathbf{x}\|_p^p \tag{3}$$

where $p < 2$ and λ are scalar parameters, and $\|\cdot\|_p$ denotes the ℓ_p-norm. The first term in the above objective function is a data fidelity term. The second term is a regularizing constraint whose role is to suppress artifacts and increase the resolvability of the scatterers in the HRR profile.

Such regularized signal reconstruction methods, based on ℓ_p-norms with $p < 2$ as in Eq. (3), or based on other non-quadratic potential functions, have been shown to provide superresolution results.[14] These methods have found use in applications such as nuclear magnetic resonance (NMR) spectroscopy,[15] astronomical imaging,[16] synthetic aperture radar (SAR) imaging,[17] and recently, source localization with passive sensor arrays.[18] These approaches achieve superresolution by exploiting the expected sparse structure of the unknown signals through the non-quadratic regularizing constraints.

We end this section by pointing out the relationship between our technique for superresolution HRR profile reconstruction and the field of adaptive signal representation.[19–21] Adaptive signal representation addresses the problem of finding optimal representations of signals as combination of elements from an overcomplete dictionary. Such techniques have been used for feature extraction from HRR profiles.[21] One adaptive signal representation technique, called basis pursuit denoising,[20] finds an optimal representation by minimizing an objective function of the same mathematical form as Eq. (3) with $p = 1$. Hence, we can interpret a special case of our signal reconstruction method as one of finding the optimal basis pursuit denoised representation of the observed HRR data, in terms of the complex exponential dictionary elements.

3.2. Algorithm

We now describe a numerical solution of the optimization problem posed in Eqs. (2) and (3). In order to avoid problems due to non-differentiability of the ℓ_p-norm around the origin when $p \leq 1$, we use a smooth approximation to the ℓ_p-norm in Eq. (3). This leads to the following slightly modified cost function to be used in practice for numerical purposes:

$$J(\mathbf{x}) = \|\mathbf{y} - \mathbf{F}\mathbf{x}\|_2^2 + \lambda \sum_{i=1}^{M} (|\mathbf{x}_i|^2 + \epsilon)^{p/2} \tag{4}$$

where $\epsilon \geq 0$ is a small constant, $\mathbf{x}_i$ denotes the i-th element of the vector $\mathbf{x}$, and M is the length of the vector $\mathbf{x}$. We minimize $J(\mathbf{x})$ by a Quasi-Newton method:

$$\hat{\mathbf{x}}^{(n+1)} = \hat{\mathbf{x}}^{(n)} - \gamma \left[\mathbf{H}\left(\hat{\mathbf{x}}^{(n)}\right)\right]^{-1} \nabla J(\hat{\mathbf{x}}^{(n)}) \tag{5}$$

where n denotes the iteration number, γ is the step size, $\nabla J(\cdot)$ is the gradient of the cost function, and $\mathbf{H}(\cdot)$ is the Hessian approximation, defined as:

$$\mathbf{H}(\mathbf{x}) \triangleq 2\mathbf{F}^H\mathbf{F} + \lambda \cdot \mathrm{diag}\left\{\frac{p}{(|\mathbf{x}_i|^2 + \epsilon)^{1-p/2}}\right\}. \tag{6}$$

Here diag$\{\cdot\}$ is a diagonal matrix whose i-th diagonal element is given by the expression inside the brackets. After substituting Eq. (6) into Eq. (5) and rearranging, we obtain our iterative algorithm:

$$\mathbf{H}\left(\hat{\mathbf{x}}^{(n)}\right)\, \hat{\mathbf{x}}^{(n+1)} = 2\mathbf{F}^H\mathbf{y} \tag{7}$$

where we have used a step size of $\gamma = 1$. We run the iteration in Eq. (7) until $\|\hat{\mathbf{x}}^{(n+1)} - \hat{\mathbf{x}}^{(n)}\|_2 / \|\hat{\mathbf{x}}^{(n)}\|_2 < \delta$, where $\delta > 0$ is a small constant.

4. EXPERIMENTAL RESULTS

In the following subsections, we present experimental results based on simple synthetic data, XPATCH-simulated[22] HRR data,[11] and HRR data extracted from stationary real SAR images.[12] These data sets have previously been used in a number of studies involving HRR profile formation and HRR ATR.[2–6] We compare the results of our method to those obtained by Capon's method[23] and RELAX,[24] as well as conventional Fourier-transform-based reconstructions. Capon's method and RELAX have played central roles in a number of recent techniques including those in Ref. 6 and Ref. 8, respectively. We discuss the potential benefits and problems associated with each approach.

4.1. Synthetic Data Reconstructions

First, we demonstrate the superresolution capability of our method on the reconstruction of a simple synthetic HRR profile composed of six scatterers, the magnitude of which is shown in Figure 1(a). This synthetic profile is much simpler than a real HRR profile since it disregards the existence of clutter and minor scatterers, however it is useful for demonstrating the behavior of the technique, and for analyzing the accuracy of the reconstructed scatterer locations based on the known truth. In our first example, the phase history data supports a resolution of 4 times worse than that of the original signal. The resolution loss is evident in the conventional, Fourier-transform-based reconstruction of Figure 1(b), where the leftmost two peaks of the original signal have been merged into one. Figure 1(c) shows the reconstruction obtained by Capon's method, where the leftmost two peaks have barely been resolved. Next, we present the result of applying RELAX. The output of RELAX is scatterer locations and the associated complex reflectivities. We provide RELAX with the true number of scatterers. In practice this number needs to be determined by using e.g. the generalized Akaike information criterion.[24] To visualize the features extracted by RELAX as a profile, we plot the estimated magnitudes of the reflectivities versus the scatterer locations in Figure 1(d). RELAX can resolve all the scatterers, although their locations are not exactly true, and the amplitudes of the scatterers relative to each other are not preserved (consider the leftmost two peaks). Finally, Figure 1(e) contains the result of the method proposed in this paper, with $p = 0.1$. All the scatterers are resolved, and the relative amplitude structure of the scatterers appears to be better preserved as compared to RELAX. As we have mentioned previously, locations of the dominant scatterers is an important feature for HRR profiles. In Table 1, we display the scatterer locations (in terms of range bins) extracted by various methods. For RELAX, these locations are an output of the technique. For the other methods, we find these locations by finding the peaks in the reconstructed HRR profile. The peaks are taken to be the points where the discrete spatial derivative of the reflectivity magnitude changes sign from positive to negative. Once the peaks are found, we order them based on their magnitudes, and pick the largest six of them. The results in Table 1 indicate that, for this particular example, Capon's method and our method find the locations perfectly, while RELAX exhibits some location errors. If we use the sum of the absolute location errors as an error criterion, RELAX has an error of 5 range bins.

In our second example, we consider a scenario where the data support a resolution that is 5.3 times worse than the original signal. As shown in Figures 2(b) and 2(c), both the conventional method, and Capon's method have difficulty resolving the scatterers in this case. RELAX and our technique provide more reasonable results as illustrated in Figures 2(d) and 2(e) in terms of resolvability. The relative amplitude structure of the original signal is better preserved by our approach as compared to RELAX. As shown in Table 2, RELAX has a localization error of 6 range bins, whereas our method can still determine the locations of all the scatterers exactly.

So far we have considered high signal-to-noise ratio (SNR) examples. Our next results are based on a similar scenario to that of Figure 2, but in this case we add a considerable amount of white Gaussian noise to the phase history data so that the SNR is 14 dB. The results are presented in Figure 3. As compared to the high-SNR case, Capon's method exhibits some loss in resolving power. Our method has a localization error of 2 range bins, while RELAX has an error of 6 range bins.

4.2. URISD Reconstructions

We now present results using the University Research Initiative Synthetic Dataset (URISD).[11] The URISD provides a collection of simulated range profiles and the associated phase histories, produced by the HRR

True peak locations	Capon's	RELAX	Proposed
120	120	119	120
122	122	121	122
140	140	140	140
143	143	144	143
178	178	177	178
182	182	183	182

Table 1: Scatterer locations extracted by various methods for the example in Figure 1.

True peak locations	Capon's	RELAX	Proposed
120	121	118	120
122	140	121	122
140	157	141	140
143	165	144	143
178	178	178	178
182	182	183	182

Table 2: Scatterer locations extracted by various methods for the example in Figure 2.

simulator XPATCH.[22] The URISD includes data for four ground vehicles (two tank models, school bus, fire truck) over three frequency bands (UHF, L, X). In the example we present here, we have used the X-band data which has a central frequency of 10 GHz, and a bandwidth of 1.4775 GHz. This implies a resolution of around 0.1 m. We have used conventionally reconstructed 0.1 m resolution profiles as the "reference" profiles. In our experiments, we have used limited data, supporting a resolution of 0.4 m to test various methods.

Figure 4(a) shows the reference profile for a fire truck at 0° orientation. The conventional reconstruction from reduced resolution data is shown in Figure 4(b). Note that the two dominant peaks around range bin 110, and the two dominant peaks around range bin 150 in the reference profile are merged into single peaks in the conventional reconstruction. As illustrated in Figure 4(c), Capon's method produces an HRR profile where the main lobes around the peaks are reduced (relative to the conventional reconstruction), however the pairs of dominant scatterers are still not resolved. For RELAX, we take the total number of scatterers to be 9. Figure 4(d) shows the RELAX result, which seems to have a better performance in terms of resolving the dominant scatterers. However some of the dominant scatterers are too much suppressed, and this might be a problem if the relative amplitude structure of the scatterers is of use for further processing. Furthermore, this might result in the missing of some of the dominant scatterers, especially if the assumed number of scatterers is not large enough. For example, if we assumed 6 scatterers in this example, RELAX would miss one of the two dominant scatterers around range bin 150.

We present two flavors of our technique in this example. First, as we did for the synthetic examples, we concentrate on extracting location features, and produce a reconstruction with $p = 0.1$, shown in Figure 4(e). This resolves the dominant scatterers, yields a similar performance to RELAX in terms of peak location accuracy, and appears to preserve the relative amplitude structure. This strategy makes sense for feature-based further processing, however there is also interest in using template-based techniques for HRR ATR,[2–6] where the entire profile serves as a feature. In this context, decision-making is done by comparing profiles at a certain resolution to templates, in terms of a similarity measure such as the mean-squared error (MSE). In our framework, we can produce reconstructions that might be useful in such a setting, while still providing reasonable resolution, by adjusting the parameter p. In Figure 4(f), we show the result of our method with $p = 1$. We believe this reconstruction is visually more "similar" to the reference profile of Figure 4(a) than any of the other reconstructions. We can quantify the similarity by computing the MSE between the reference profile and various reconstructed profiles. The MSEs are $33.5 \cdot 10^{-3}$ for the conventional method, $18.8 \cdot 10^{-3}$ for RELAX, $6.29 \cdot 10^{-3}$ for our method with $p = 0.1$, and $4.77 \cdot 10^{-3}$ for our method with $p = 1$. This suggests that the proposed technique can be tailored to the nature of further processing.

True peak locations	Capon's	RELAX	Proposed
120	9	118	120
122	96	121	122
140	121	141	140
143	141	144	144
178	179	178	178
182	183	183	183

Table 3: Scatterer locations extracted by various methods for the example in Figure 3.

4.3. MSTAR Data Reconstructions

We now show results on data from the Moving and Stationary Target Acquisition and Recognition (MSTAR) public target data set.[12] The MSTAR public target data set provides SAR images of various military vehicles. The phase history data used in our experiments are obtained from the SAR images by undoing the image formation process. The MSTAR images have a resolution of around 0.3 m. In our experiments we have used limited phase history data, supporting a resolution of 1.2 m. The results for a BTR70 vehicle, presented in Figure 5, are very similar qualitatively and quantitatively to the URISD example presented in Section 4.2. For RELAX, we set the number of scatterers to 5 in this example.

5. POTENTIAL EXTENSIONS AND TOPICS FOR FUTURE ANALYSIS

The work in this paper is quite preliminary, and we would like to mention a number of issues, potential extensions, and experimental analyses that might be the subject of future research.

One issue with the proposed method (as with most regularization-based methods) is the choice of parameters (in our case p and λ). In the work presented here, we have chosen these parameters by subjective assessment, based on the goals of the processing. In a practical setting, one needs a principled, automatic way to choose these parameters. This is important for effective use of the framework presented.

We want to mention two potential extensions of the technique. First, the framework is not limited to the use of ℓ_p-norms in the regularizing constraints, and other non-quadratic potential functions can certainly be used. Second, the framework can be generalized to enhance features other than dominant scatterer locations. For example, if the length of the target is the feature that will be used in ATR, one may extend the framework to use a regularizing constraint that will accentuate this type of feature in the HRR profile.

A more detailed performance analysis of the method is needed. Our experiments were on a small number of profiles, and an evaluation of the technique in terms of feature extraction accuracy on a large data set would be useful. Another valuable analysis would be the investigation of the impact of our reconstructions on HRR ATR.

6. CONCLUSIONS

We have demonstrated the use of a non-quadratic regularization technique for superresolution and feature-enhanced reconstruction of HRR profiles. Our experimental work suggests that the method can produce higher resolution profiles than Capon's method, and can extract features with comparable or higher accuracy than RELAX. The framework is flexible in the sense that, through the choice of a parameter, one can focus on extraction of range features, or alternatively on the formation of a typical profile at a certain resolution. In an ATR setting, this flexibility can be used to tailor the technique to the nature of the recognition processing.

ACKNOWLEDGMENTS

This work was supported by the Army Research Office under Grants DAAD19-00-1-0466 and DAAG55-97-1-0013, the Office of Naval Research under Grant N00014-00-1-0089, the Air Force Office of Scientific Research under Grant F49620-96-1-0028, and the National Institutes of Health under Grant NINDS 1 R01 NS34189.

REFERENCES

1. R. A. Mitchell and J. J. Westerkamp, "Robust statistical feature based aircraft identification," *IEEE Trans. Aerosp. Electron. Syst.* **35**, pp. 1077–1094, July 1999.
2. R. Williams, J. Westerkamp, J. Gross, and A. Palomino, "Automatic target recognition of time critical moving targets using 1D high range resolution (HRR) radar," *IEEE Aerospace and Electronic Systems Magazine* **15**, pp. 37–43, Apr. 2000.
3. S. P. Jacobs and J. A. O'Sullivan, "High resolution radar models for joint tracking and recognition," in *Automatic Target Recognition VII*, F. A. Sadjadi, ed., *Proc. SPIE* **3069**, pp. 94–105, 1997.
4. S. P. Jacobs and J. A. O'Sullivan, "Automatic target recognition using sequences of high resolution radar range-profiles," *IEEE Trans. Aerosp. Electron. Syst.* **36**, pp. 364–382, Apr. 2000.
5. D. H. Nguyen, G. R. Benitz, J. H. Kay, and R. H. Whiting, "Super-resolution HRR ATR performance with HDVI," in *Automatic Target Recognition X*, F. A. Sadjadi, ed., *Proc. SPIE* **4050**, (Orlando, FL, USA), Apr. 2000.
6. D. Nguyen, G. Benitz, J. Kay, B. Orchard, and R. Whiting, "Superresolution HRR ATR with high definition vector imaging," *IEEE Trans. Aerosp. Electron. Syst.* **37**, pp. 1267–1285, Oct. 2001.
7. G. Liu, H. Li, and J. Li, "Moving target feature extraction with polarisation diversity in the presence of arbitrary range migration and phase errors," *IEE Proc. Radar, Sonar and Navigation* **147**, pp. 208–216, Aug. 2000.
8. J. Li, G. Liu, N. Jiang, and P. Stoica, "Moving target feature extraction for airborne high-range resolution phased-array radar," *IEEE Trans. Signal Processing* **49**, pp. 277–289, Feb. 2001.
9. N. Jiang, R. Wu, and J. Li, "Super resolution feature extraction of moving targets," *IEEE Trans. Aerosp. Electron. Syst.* **37**, pp. 781–793, July 2001.
10. Z. Bi, R. Wu, J. Li, and R. Williams, "Joint super-resolution moving target feature extraction and stationary clutter suppression," *IEE Proc. Radar, Sonar and Navigation* **147**, pp. 23–29, Feb. 2000.
11. "Center for Imaging Science URISD Web Page: http://cis.jhu.edu/wu_sensor_data/urisd/."
12. "Air Force Research Laboratory, Model Based Vision Laboratory, Sensor Data Management System MSTAR Web Page: http://www.mbvlab.wpafb.af.mil/public/sdms/datasets/mstar/."
13. G. R. Benitz, "High-definition vector imaging," *Lincoln Laboratory Journal* **10**(2), pp. 147–170, 1997.
14. D. L. Donoho, I. M. Johnstone, J. C. Koch, and A. S. Stern, "Maximum entropy and the nearly black object," *J. R. Statist. Soc. B* **54**(1), pp. 41–81, 1992.
15. S. Sibisi, J. Skilling, R. G. Brereton, E. D. Laue, and J. Staunton, "Maximum entropy signal processing in practical NMR spectroscopy," *Nature* **311**, pp. 446–447, Oct. 1984.
16. R. Narayan and R. Nityananda, "Maximum entropy restoration in astronomy," *Ann. Rev. Astron. Astrophys.* **24**, pp. 127–170, 1986.
17. M. Çetin and W. C. Karl, "Feature-enhanced synthetic aperture radar image formation based on non-quadratic regularization," *IEEE Trans. Image Processing* **10**, pp. 623–631, Apr. 2001.
18. D. M. Malioutov, M. Çetin, J. W. Fisher III, and A. S. Willsky, "Super-resolution source localization through data-adaptive regularization," in *Adaptive Sensor Array Processing Workshop*, (Lexington, MA, USA), Mar. 2002.
19. S. Mallat and Z. Zhang, "Matching pursuits with time-frequency dictionaries," *IEEE Trans. Signal Processing* **41**(12), pp. 3397–3415, 1993.
20. S. S. Chen, *Basis Pursuit*. PhD thesis, Stanford University, 1995.
21. S. Jaggi, W. C. Karl, H. Krim, S. Mallat, and A. S. Willsky, "Feature extraction through high-resolution pursuit," *Applied and Computational Harmonic Analysis* **5**, 1998.
22. M. Hazlett, D. J. Andersh, S. W. Lee, H. Ling, and C. L. Yu, "XPATCH: a high-frequency electromagnetic scattering prediction code using shooting and bouncing rays," in *Targets and Bachgrounds: Characterization and Representation*, W. R. Watkins and D. Clement, eds., *Proc. SPIE* **2469**, pp. 266–275, (Orlando, FL, USA), Apr. 1995.
23. J. Capon, "High resolution frequency-wavenumber spectrum analysis," *Proc. IEEE* **57**(8), pp. 1408–1418, 1969.
24. J. Li and P. Stoica, "Efficient mixed-spectrum estimation with applications to target feature extraction," *IEEE Trans. Signal Processing* **44**, pp. 281–295, Feb. 1996.

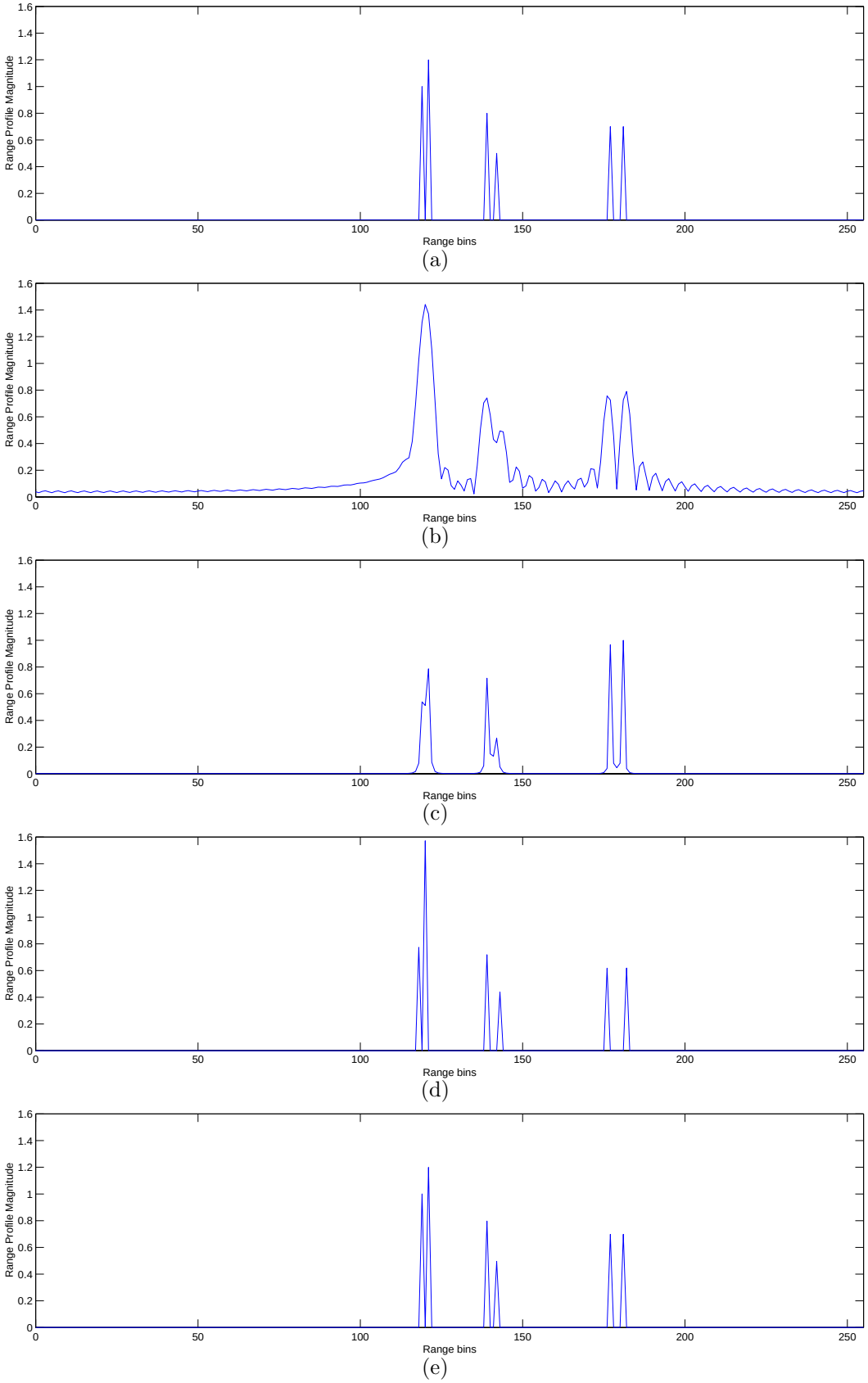

Figure 1. Synthetic HRR profile reconstruction. Data supports a resolution of 4 times worse than that of the original signal. (a) True profile. (b) Conventional reconstruction. (c) Capon's method. (d) RELAX. (e) Proposed method with $p = 0.1$.

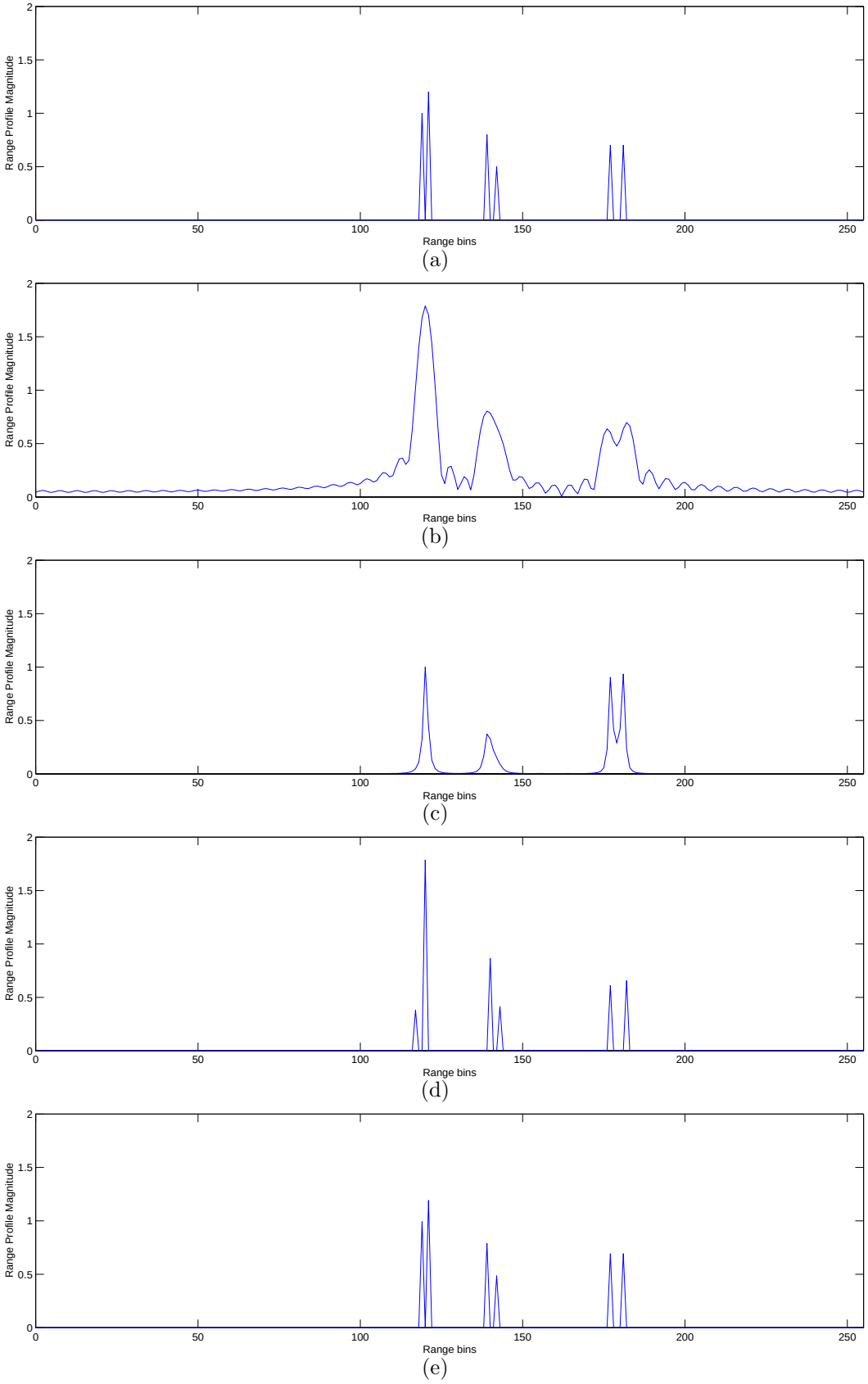

Figure 2. Synthetic HRR profile reconstruction. Data supports a resolution of 5.3 times worse than that of the original signal. (a) True profile. (b) Conventional reconstruction. (c) Capon's method. (d) RELAX. (e) Proposed method with $p = 0.1$.

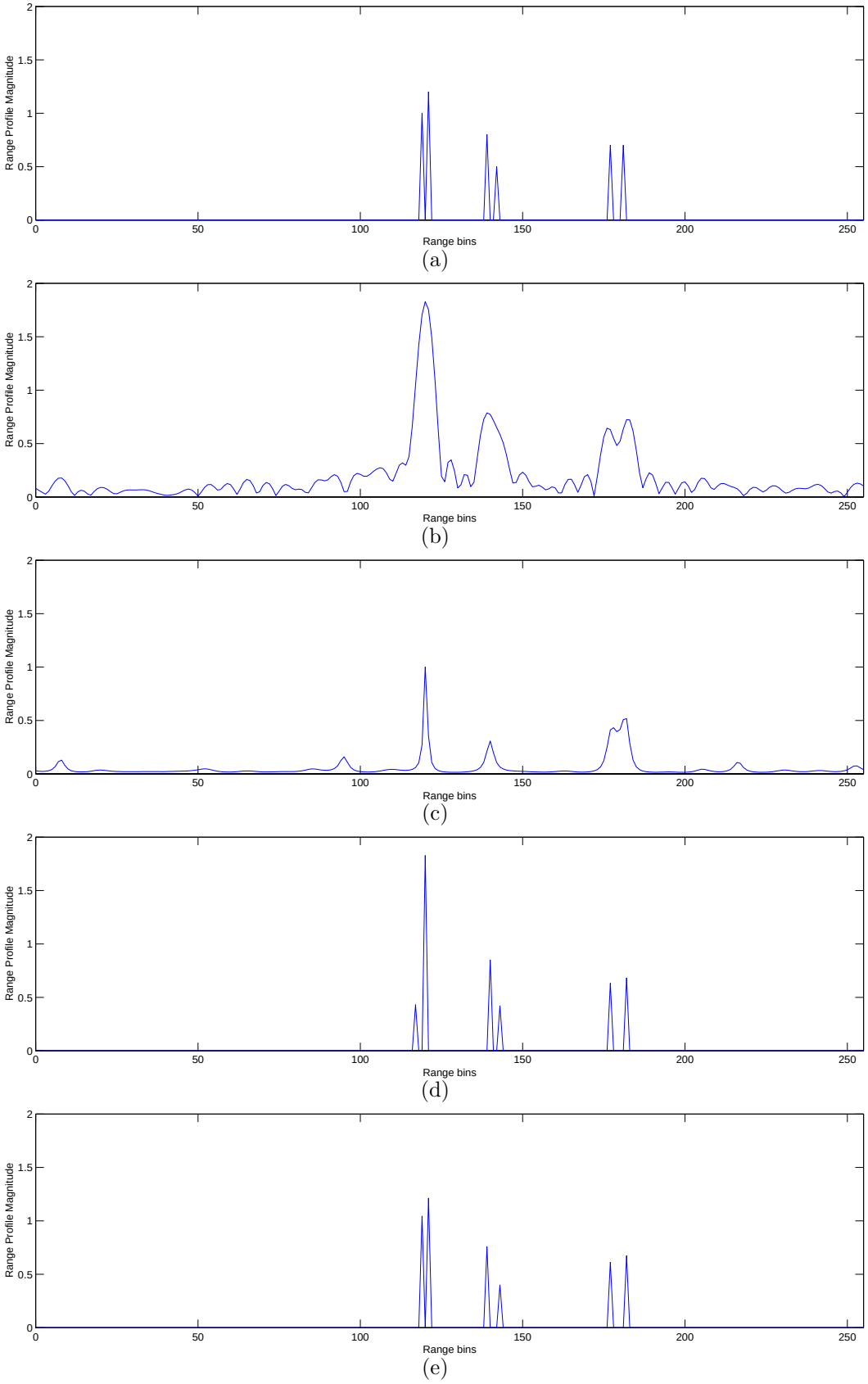

Figure 3. Synthetic HRR profile reconstruction from low-SNR (14 dB) data. Data supports a resolution of 5.3 times worse than that of the original signal. (a) True profile. (b) Conventional reconstruction. (c) Capon's method. (d) RELAX. (e) Proposed method with $p = 0.1$.

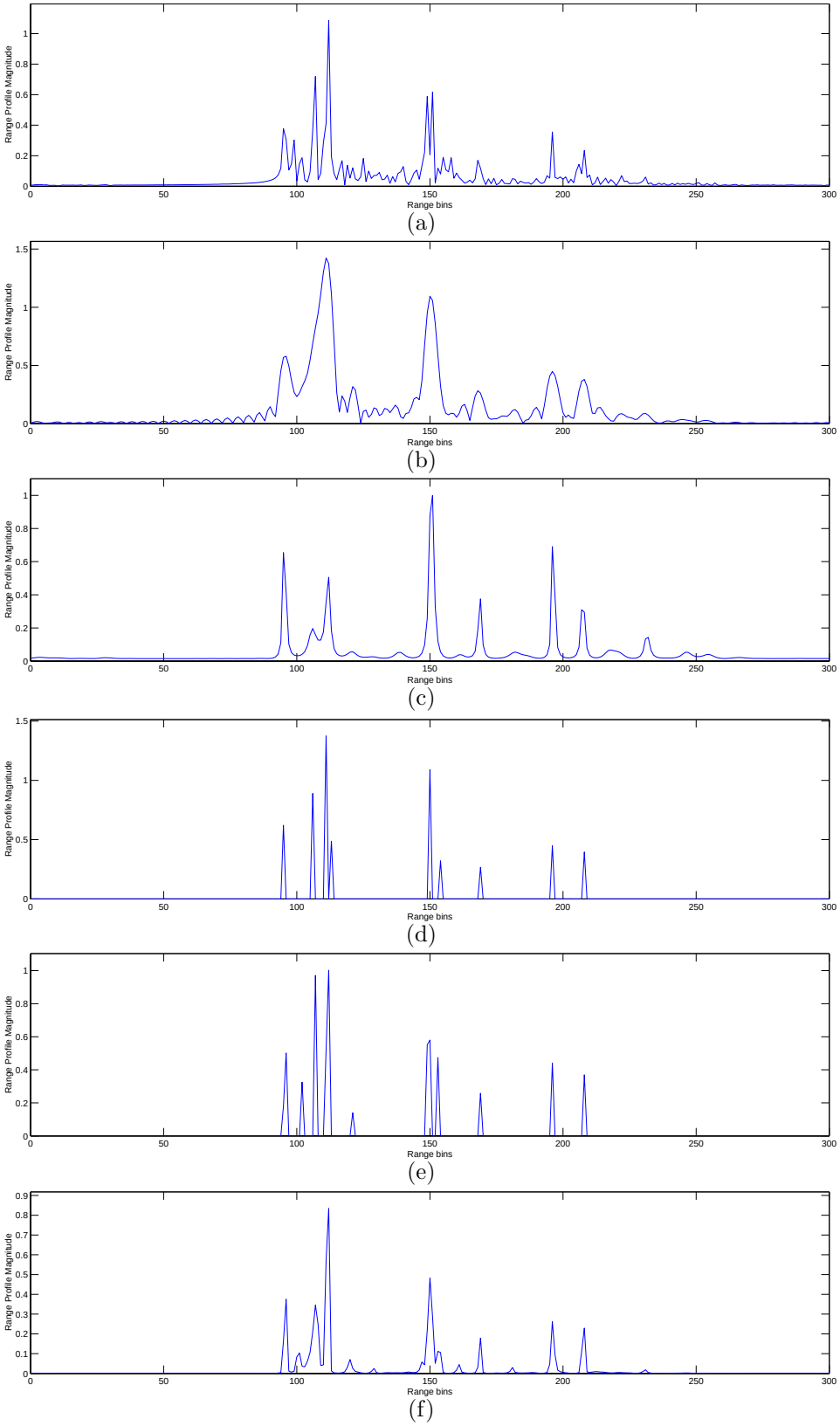

Figure 4. HRR profiles of a fire truck from the URISD at 0° orientation. Reconstructions use 0.4 m resolution data. (a) Reference profile at 0.1 m resolution. (b) Conventional reconstruction. (c) Capon's method. (d) RELAX. (e) Proposed method with $p = 0.1$. (f) Proposed method with $p = 1$.

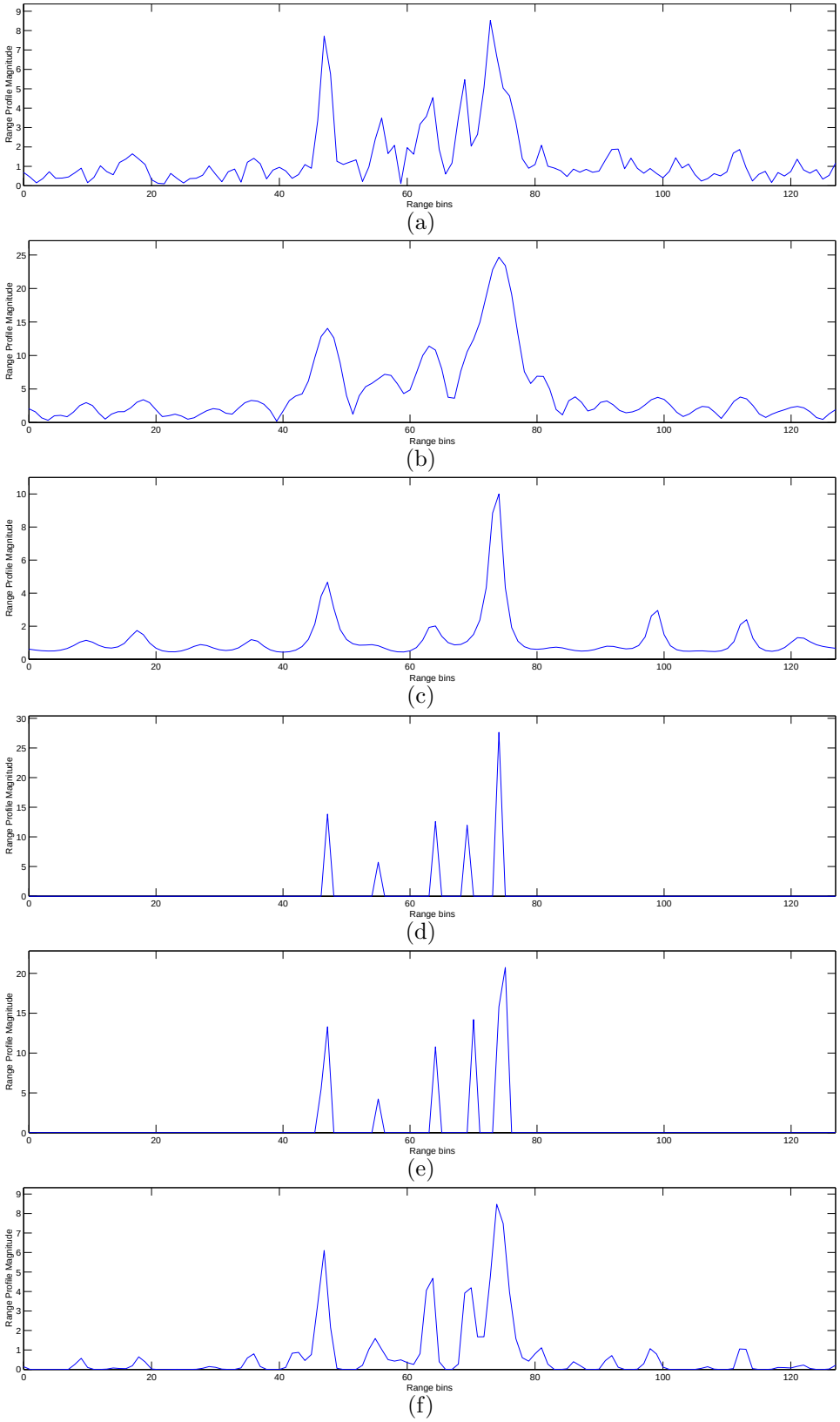

Figure 5. HRR profiles of a BTR70 armored personnel carrier from the MSTAR data set. Reconstructions use 1.2 m resolution data. (a) Reference profile at 0.3 m resolution. (b) Conventional reconstruction. (c) Capon's method. (d) RELAX. (e) Proposed method with $p = 0.1$. (f) Proposed method with $p = 1.1$.